Abstract # 475

Understanding the role of tumor immune microenvironment in determining response to Immune Checkpoint Inhibitor in Colorectal Cancer

Dharanidharan M[1], Biswajit Das[1], Kowshik Jaganathan[1], Syamkumar V[1], Chandan Bhowal[1], Mouniss MM[1], Saikrishna S[1], Abdul Haseeb[1], Moumita Nath[1], Jobin K[1], Vasanthakumar A[1] , Rajashekar M[1], Oliyarasi M[1], Priyanka Chevour[1], Mehul Kapur[1], Jayaprakash C[3], MS Ganesh[4], Amritha Prabha[4], Prakash BV[5], Upendra K[1], Ritu Malhotra[1], Govindaraj K[1], Pavithira[1], Mohit Malhotra[2], Satish Sankaran[1,#,*]

[1]Farcast Biodynamics India Pvt. Ltd., Bangalore, [2]Farcast Biodynamics LLC, Pensacola, FL USA, [3]DBR & SK Super Speciality Hospital, Tirupati, [4]Vydehi Institute of Medical Sciences and Research Centre, Bangalore, [5]Sri Lakshmi Multi Speciality Hospital, Bangalore, [#]Presenting and *corresponding author

Background

Colorectal cancer (CRC) is a significant global health issue. Response rate to immune checkpoint inhibitors (ICI) in MSI-H CRC patients have been encouraging but highly variable, pointing to the need for a better response biomarker for patient selection. We employed the Farcast CRC TruTumor histoculture platform to understand the role and response of immune cell types in the complex Tumor MicroEnvironment (TME) that could identify ICI therapy responders more accurately.

Methods

Patient tissue samples: Fresh, surgically resected CRC tissue samples (n=6) were collected from consented patients along with matched blood.

Histo-Culture workflow: Tumor samples were processed to generate thin explants with vibratome, without enzymatic digestion, to retain the native tumor microenvironment. Tumor explants were distributed into treatment arms and cultured for 72 h with media replenished every 24h. Response to T-cell stimulation with anti-CD3 (100 ng/mL) + Interleukin-2 (IL-2, 100 IU/mL) and treatment with Nivolumab (132 µg/mL) was evaluated using cytokine release and flow cytometry based immune profiling.

Cytokine Analysis: The culture supernatants were collected every 24h. Supernatants pooled from all time points were evaluated for the presence of cytokines, namely IL10, TNF-a, IFN-g, Granzyme B and Perforin, using Luminex MAGPIX instrument and data was analysed using MILLIPLEX™ Analyst software.

Flow cytometry analysis: Post culture, tumor explants were dissociated to generate a single cell suspension, followed by staining with Live/Dead dye and a cocktail of antibodies for immune cell lineage and activation. Data was acquired using BD LSR Fortessa flow cytometer with appropriate compensation controls and analyzed using FlowJo software.

Statistical analysis: All data analysis and graphical representations were done using GraphPad Prism (Version 10.1.1). Mann-Whitney t-test was used to generate p-values. p-value significance is represented as *(p≤0.05) **(p≤0.01) ***(p≤0.01). Heat maps were generated on GraphPad and Morpheus (https://software.broadinstitute.org/Morpheus).

Study Design

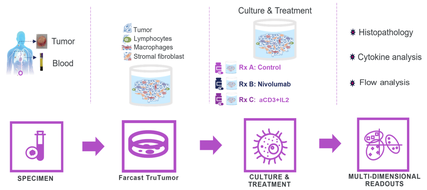

Fig. 1: Schematic representation of Farcast™ TruTumor Histoculture platform work-flow and downstream assays used for treatment response evaluation.

Patient demography

Parameters	Categories	Values %
Median age	≤55	3 (50%)
	>55	3 (50%)
Gender	Female	5 (83.3%)
	Male	1 (16.7%)
Tumor stage	I	0 (0%)
	II	2 (33.3%)
	III	2 (33.3%)
	IV	2 (33.3%)
Grade	Grade 1	1 (16.7%)
	Grade 2	3 (50%)
	Grade 3	2 (33.3%)
Primary/ Recurrent	Primary	6 (100%)
Tumor site	Rectum	1 (16.7%)
	Recto sigmoid	1 (16.7%)
	Transverse colon	2 (33.3%)
	Caecum	2 (33.3%)

Table 1: Demography of patient samples (n=6) used for the study

Results

CRC comprised an immunosuppressive microenvironment at baseline compared to other indications

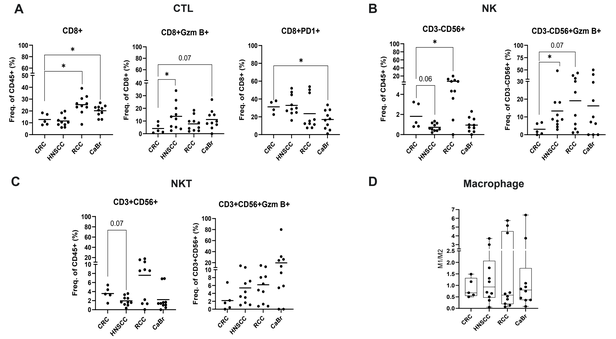

Fig. 2: Comparison of tumor immune microenvironment across indications (A) Difference in the various CTL (CD8+T cell) sub-population (B) NK cell sub-populations (C) NKT cell sub-populations and (D) M1/M2 macrophage ratio across four different cancer indications

CRC exhibited a muted response to T-cell stimulation with Anti-CD3+IL2 compared to other indications

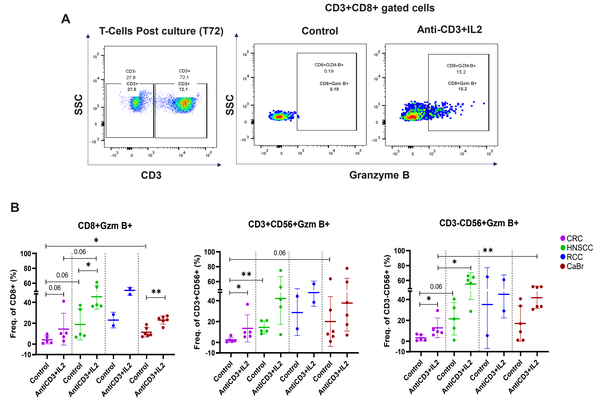

Fig. 3: T cell stimulation with Anti-CD3 and IL2 (A) Evaluation of activated T-cell proportion in CRC samples (B) Effect on activation of various effector cell populations across indications: CRC (n=5), HNSCC (n=5), RCC (n=2) and CaBr (n=6)

Nivolumab treatment response in CRC is negatively affected by immunosuppressive environment in CRC

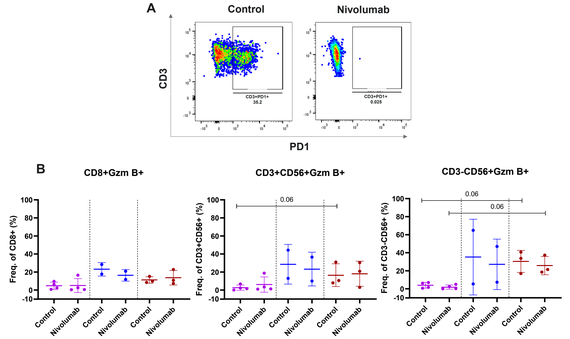

Fig. 4: (A) Flowcytometry data showing masking of PD1 receptor in nivolumab treated arm (B) Change in proportions of activated effector immune cells across 3 indications, RCC (n=2) and CaBr (n=3) and CRC (n=4), upon Nivolumab treatment

Strong T-cell reinvigoration phenotype observed in Nivolumab-responsive CRC sample (S6)

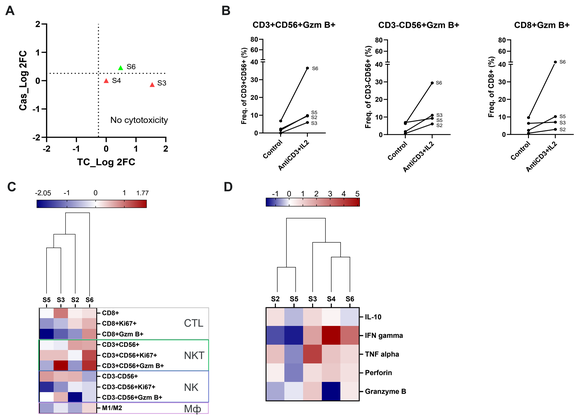

Fig. 5: Immune profiling of CRC samples post-Nivolumab (A) Two-dimensional dot plot representation of Log2 FC in tumor content and cleaved caspase 3 expression in tumor highlights cytotoxic effect (B) Proportions of CD3+CD56+GzmB+, CD3-CD56+GzmB+, and CD8+GzmB+ cells following anti-CD3 and IL-2 stimulation (C) Heatmap showing post-treatment Log2 fold-change of immune subsets, including CD8+GzmB+, CD3+CD56+GzmB+, CD3-CD56+Gzm B+ cells, and the M1/M2 ratio (D) Cytokine profiles (IL10, IFN-γ, TNF-α, Perforin and Granzyme B) across samples S3, S4, and S6

Proportions of tumor-informed activated CD8+ T cells (CD8+PD1+Gzm B+) determine response to Nivolumab

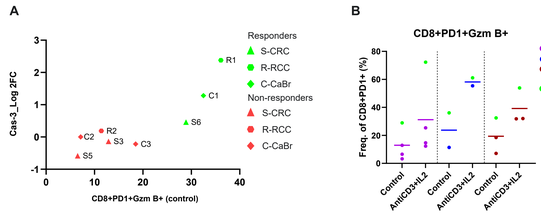

Fig. 6: (A) Two-dimensional dot plot illustrating the relationship between baseline CD8+PD1+Gzm B+ (control arm) and caspase-3 Log2 FC in CRC, RCC, and CaBr samples after Nivolumab treatment (B) Proportions of tumor-informed T cells across different indications (CRC, RCC, and CaBr) following anti-CD3 and IL2 stimulation

Nivolumab responder S6 has higher level of total and tumor infiltrated CD8+T cells in absence of treatment

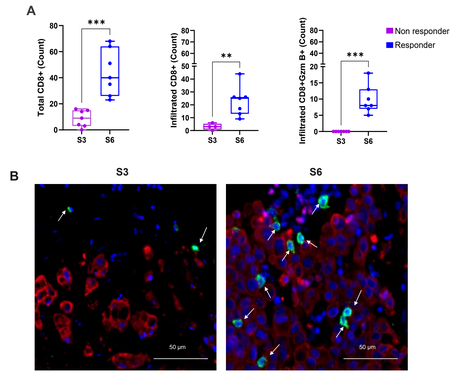

Fig. 7: (A) Box-and-whisker plot illustrating the distribution of infiltrated and activated CD8+ T cells in responder (S6) and non-responder (S3) (B) Representative multiplex IHC images depicting cytotoxic T lymphocytes (CTLs) within the tumor nests of responder and non-responder samples

Conclusions

- The TruTumor platform reproduced the immunosuppressive TME in CRC.
- Data points to the presence of dysfunctional or irreversibly exhausted CTLs that restricts the efficacy of ICI monotherapy.
- The platform provides the opportunity to explore combination therapy strategies to overcome the shortcoming of ICI monotherapy for better outcomes.

Email: biopharma@farcastbio.com